Analytical Methods

A Fe3O4@SiO2@polypyrrole magnetic nanocomposite for the extraction and preconcentration of Cd(II) and Ni(II)

Journal:	*Analytical Methods*
Manuscript ID:	AY-ART-08-2014-001991.R2
Article Type:	Paper
Date Submitted by the Author:	03-Oct-2014
Complete List of Authors:	Abolhasani, Jafar; Tabriz Branch, Islamic Azad University, Hosseinzadeh khanmiri, Rahim; Islamic Azad University, Ghorbani-Kalhor, Ebrahim; Tabriz Branch, Islamic Azad University, Asgharinezhad, Ali Akbar; Young Researchers and Elite Club, Karaj Branch, Islamic Azad University, Chemistry Shekari, Nafiseh; Young Researchers and Elite Club, Karaj Branch, Islamic Azad University, Chemistry Fathi, Ahoura; Department of Mathematical Sciences, Sharif University of Technology,

A Fe_3O_4@SiO_2@polypyrrole magnetic nanocomposite for the extraction and preconcentration of Cd(II) and Ni(II)

Jafar Abolhasani [a,*], Rahim Hosseinzadeh Khanmiri [a], Ebrahim Ghorbani-Kalhor[a], Ali Akbar Asgharinezhad [b], Nafiseh Shekari [b], Ahoura Fathi[c]

[a] *Department of Chemistry, College of Science, Tabriz Branch, Islamic Azad University, Tabriz, Iran,*

[b] *Young Researchers and Elite Club, Karaj Branch, Islamic Azad University, P.O. Box 31485-313, Karaj, Iran*

[c] *Department of Mathematical Sciences, Sharif University of Technology, Tehran, Iran*

* Corresponding author: Fax: +98 4113333458; Tel: +98 9141028230
E-mail: Abolhasani@iaut.ac.ir (J. Abolhasani)

Abstract

This work describes a novel Fe_3O_4@SiO_2@polypyrrole magnetic nanocomposite and its application in the preconcentration of Cd(II) and Ni(II) ions. The parameters affecting the preconcentration procedure were optimized by a Box-Behnken design through response surface methodology. Three variables (extraction time, magnetic sorbent amount, and pH value) were selected as the main factors affecting the sorption step, while four variables (type, volume and concentration of the eluent; and elution time) were selected as main factors in the optimization study of the elution step. Following the sorption and elution of analytes, the ions were quantified by FAAS. The limits of detection were 0.3 and 1.2 ng mL^{-1} for Cd(II) and Ni(II) ions, respectively. All the relative standard deviations were less than 8.8%. The obtained sorption capacities (in mg g^{-1}) of this new sorbent are 120 for Cd(II) and 98 for Ni(II). Ultimately, this nanocomposite was successfully applied to the rapid extraction of trace quantities of heavy metal ions from sea food samples and satisfactory results were obtained.

***Keywords*:** Functionalized Fe_3O_4@SiO_2 core-shell nanoparticles; Cd(II); Ni(II); Sorption; Response surface methodology; Box-Behnken design.

1. Introduction

Heavy metal ions are toxic pollutants which exist in different samples and their presence concerns industries and environmental organizations all over the world. Most of these pollutants are very toxic and dangerous for human health. Thus the determination of trace amounts of heavy metals is often a major task for analytical chemists, as it is a good tool for the monitoring and identification of toxicants in environmental samples. Among heavy metals which exist in the environment, cadmium monitoring is very crucial due to the fact that cadmium concentration in the environment is increasing dramatically.[1,2] Cadmium exposure can be linked to diseases associated with aging such as osteoporosis, prostate, and pancreatic cancer.[3,4] Another heavy metal which is also toxic is nickel. Aspirating cadmium derivatives can lead to serious problems, including nasopharynx, lung and dermatological diseases and malignant tumors. Moreover, nickel can cause skin disorder, known as nickel-eczema which is a considerable health problem exclusively among women.[5] It has been proven to be a carcinogenic agent. Various instrumental techniques, including electrothermal atomic absorption spectrometry (ETAAS),[6,7] inductively coupled plasma-optical emission spectrometry (ICP-OES),[8] flame atomic absorption spectrometry (FAAS),[9] inductively coupled plasma-mass spectrometry (ICP-MS),[10] and total reflection XRF-spectrometry,[11] have been used for the determination of heavy metals. Since the heavy metals' concentration level in environmental samples is fairly low and the complexity of matrices is the main problem; thus preconcentration techniques are often required.[12] Various procedures such as liquid-liquid extraction (LLE),[13] cloud point extraction,[14] chemical precipitation,[15] ion exchange,[16] and solid phase extraction (SPE) have been developed for the extraction and preconcentration of heavy metals in natural matrices.[17-19]

Among the aforementioned methods, the most commonly used technique for the preconcentration of heavy metal ions from environmental samples is solid phase extraction. Widespread application of SPE is due to its intrinsic simplicity, rapidity, minimal cost, and low consumption of reagents.[20] By the advent of SPE, diverse sorbents such as carbon nanotubes,[21-24] magnetic nanoparticles,[25] solid sulfur,[26] cotton,[27] and modified porous materials [28,29] have been utilized.

In recent years, great attention has been devoted to the application of nano-structure materials in analytical chemistry, especially magnetic nanoparticles. [30-32] Magnetic Fe_3O_4 nanoparticles (Fe_3O_4 NPs) are a special kind of nano-sized materials which exhibit magnetic property besides the general features of nanometer-sized materials. However, naked Fe_3O_4 nanoparticles tend to aggregate, prone to be oxidized, and are not selective toward complex matrices. Hence, the surface of these magnetic nanoparticles has been modified with a specific ligand which turns them into a selective and appropriate sorbent. Another approach to this problem is core-shell nanostructures. Fe_3O_4 NPs are one of the most generally used nanostructures as a core to synthesis core-shell systems due to their strong super paramagnetic properties. Silica is one of the most ideal shells due to its several unique advantages: (a) silica shell prevents Fe_3O_4 NPs from aggregation in wide pH ranges and improves their chemical stability, (b) silica surface is often terminated by silanol groups that can react with silane coupling agents in order to conjugate with a variety of specific ligands and (c) the SiO_2 layers possess a good hydrophilicity behavior.[33] According to the hard and soft acid and base theory (HSAB), soft acids like most of heavy metals react faster and form stronger bonds with ligands containing N and S moieties.[34]

In a previous work yolk/shell composites with a movable Fe_3O_4 core inside the hollow polypyrrole (PPy) capsules were obtained through a template-assistant selectively etching

method. Yolk/shell Fe_3O_4@PPy composites were used as supports for deposition of Pd NPs. Finally, Fe_3O_4@PPy/Pd catalysts were used in the reduction of methylene blue dye with sodium borohydride as reducing agent.[35] In another work, a high-magnetic heavy-metal ion adsorbent which comprises a Fe_3O_4 polycrystal sphere cluster, an amorphous SiO_2 protective layer and a polypyrrole adsorption outer layer, from inside to outside, was synthesized. [36]

In this work, Fe_3O_4@SiO_2@polypyrrole magnetic nanocomposite has been utilized as a novel sorbent for the fast separation and preconcentration of Cd(II) and Ni(II) ions in various matrices. In reference 36, $FeCl_3$ was used as an oxidizing agent for the oxidative polymerization of pyrrole but we used ammonium peroxydisulfate in 1.0 mol L^{-1} HCl solution for polymerization step and the two Fe_3O_4 NPs synthesis procedures are completely different. In the previous work solvothermal method was used for Fe_3O_4 NPs synthesis, but we applied a coprecipitation rout for Fe_3O_4 NPs synthesis which is an easier and time-saving method compared to solvothermal rout. This sorbent was characterized by Fourier transform infrared spectroscopy (FT-IR), elemental analysis, transmission electron microscopy (TEM), X-ray diffraction (XRD) and scanning electron microscopy (SEM). The magnetic property of the sorbent provides a rapid and easy separation of the new solid phase from the solution. The modification of the sorbent helps it to show selectivity towards these heavy metals. Also nanometer characteristics would enhance the surface area and sorption capacity of this new sorbent. A Box–Behnken design was used in order to explore the optimum conditions of this method through response surface methodology. Finally, the nanosorbent was used for the preconcentration and determination of Cd(II) and Ni(II) ions in different sea samples and satisfactory results were obtained.

2. Experimental

2.1. Reagents and solutions

All reagents of analytical grade (pyrrole (Py), $FeCl_2$, $FeCl_3$, HCl, HNO_3, NaOH, KCl, ammonium hydroxide (25%), and tetraethyl orthosilicate (TEOS), ammonium peroxydisulfate (APS), ethanol, methanol ethanol, and acetone) were purchased from Merck (Darmstadt, Germany) or from Fluka (Seelze, Germany) and were used without further purification. Standard solutions of 1000 mg L^{-1} of Cd(II) and Ni(II) were purchased from Merck. All solutions were prepared using double distilled water.

2.2. Instrumentation

An AA-680 Shimadzu (Kyoto, Japan) flame atomic absorption spectrometer with a deuterium background corrector was used for the determination of Cd(II) and Ni(II) ions. Cadmium and nickel hollow cathode lamps (HCL) were used as the radiation sources with wavelengths of 228.8 and 232.0 nm, respectively. All measurements were carried out in an air/acetylene flame. The pH of the solutions were measured at 25 ± 1 ºC with a digital WTW Metrohm 827 Ion analyzer (Herisau, Switzerland) equipped with a combined glass-calomel electrode. CHN analysis was performed by a Thermo Finnigan Flash EA112 elemental analyzer (Okehampton, UK). IR spectra were recorded by a Bruker IFS-66 FT-IR Spectrophotometer (Bruker). Scanning electron microscopy (SEM) was performed by gently distributing the sample powder on the stainless steel stubs, using an SEM (KYKY- 3200, Beijing, China) instrument. Transmission electron microscopy (TEM) analyses were performed by a LEO 912AB electron microscope (Leo Ltd., Germany). X-ray diffraction (XRD) pattern was obtained with a Philips-PW 12C diffractometer (Amsterdam, the Netherlands) using Cu Kα radiation.

2.3. Preparation of standard solutions

Standard reference material was digested with 6 mL of HCl (37% (v/v)) and 2 mL of HNO_3 (65% (v/v)) in a microwave digestion system. Digestion was carried out for 2 min at 250 W, 2 min at 0 W, 6 min at 250 W, 5 min at 400 W, 8 min at 550 W, and then venting for 8 min. The digestion residue was then diluted with double distilled water.[37] Standard Stock solutions (1000 mg L^{-1}) of K^+, Na^+, Ca(II), Mn(II), Mg(II), Hg(II), Co(II), Zn(II), Ni(II), Fe(III), Cr(III), Cu(II), Al(III), AsO_4^{3-} and CrO_4^{2-} were prepared in a 2% (v/v) HNO_3 solution. The mixed working standard solutions were prepared by diluting an appropriate amount of the stock solution with double distilled water. All of these solutions were stored at ambient temperature.

2.4. Synthesis of Fe_3O_4@SiO_2@polypyrrole magnetic nanocomposite

2.4.1. Synthesis of Fe_3O_4@ SiO_2 core-shell nanoparticles

Fe_3O_4 NPs were synthesized according to our previously reported procedure.[29] Then 1.0 g of synthesized Fe_3O_4 NPs were dispersed in a solution of 200 mL deionized water, 50 mL ethanol and 3.0 mL NH_4OH (25%). In the next step, a total amount of 2.5 mL TEOS was added dropwise to the mixture under vigorous stirring in order to obtain the Fe_3O_4@SiO_2 core-shell NPs.[38] After 12 h stirring at 40˚C, the Fe_3O_4@SiO_2 NPs were separated by a strong magnet, washed with ethanol and then dried at room temperature (Fig. 1).

2.4.2. Modification of Fe_3O_4@ SiO_2 nanoparticles by polypyrrole

The procedure for modifying Fe_3O_4@SiO_2 core-shell nanoparticles includes two steps as follows: In the first step, 1.0 g of Fe_3O_4@SiO_2 NPs was suspended in 150 mL of HCl 1 mol L^{-1} solution and sonicated for 15 min. Then 1.0 mL of pyrrole was added into the reaction mixture and stirred for 30 min. The solution was then cooled to 0 °C, and a stoichiometric amount of APS, in 1 mol L^{-1} HCl solution, was added dropwise to the reaction mixture and polymerization was continued for 10 h and finally, a precipitate was obtained.[39] Afterward, the Fe_3O_4@SiO_2@PPy nanocomposite were separated by a strong magnet and washed with methanol and water several times in order to discard any impurities and then dried at room temperature. A schematic diagram for the synthesis of Fe_3O_4@SiO_2@PPy nanocomposite is depicted in Fig. 1.

2.5. Sorption and elution step

Extracting Cd(II) and Ni(II) ions from aqueous solutions was investigated in batch mode analysis. The sorption step was performed in test tubes containing 25 µg of Cd(II) and Ni(II) ions in 50 mL of double distilled water. According to the preliminary experimental design, the pH of the solutions was adjusted by the dropwise addition of 1.0 mol L^{-1} NH_3 and 1.0 mol L^{-1} HCl. Then the magnetic sorbent was added into the solutions. Afterward, the mixture was stirred for an appropriate amount of time in order to extract these heavy metal ions from the solution completely. Finally, the test tubes were exposed to a strong magnet (15 cm × 12 cm × 5 cm, 1.4 T), where permanent magnet in the wall caused the sorbent to aggregate on one side of the test tube. The sorbed amount of Cd(II) and Ni(II) ions were determined using FAAS due to their concentration change in solution after the sorption procedure was completed. The instrument's

response was periodically checked with known Cd(II) and Ni(II) ions standard solutions. Extraction percentage for each ion was calculated using the following equation:

$$\textbf{Extraction}\% = \frac{\mathbf{C_A - C_B}}{\mathbf{C_A}} \times \mathbf{100}$$

where C_A and C_B are initial and final concentration (mg L^{-1}) of each ion in the solution, respectively. In the elution step, 7.5 mL of a 1.5 mol L^{-1} HNO_3 solution was added to the magnetic sorbent as an eluent and the solution was shaken. This mixture was again exposed to the strong magnet and the clear solution, containing the eluted heavy metal ions was introduced to FAAS in order to determine the amount of each ion.

2.6. Real sample pretreatment

2.6.1. Fish and shrimp samples

Fish samples were collected from Caspian Sea, Siahroud River and two different sites in Moosa creek. Moosa creek is located in the Northwest of the Persian Gulf (in the south of Iran), and has several subsidiary creeks. Among them, Jafar creek was chosen as a polluted site and Behad creek as a reference site since it is far from petrochemical industries. The shrimps and canned tuna were purchased from local supermarkets in Tehran, Iran. The river fish was collected from Siahroud River (Gilan Province in the North of Iran). The fish samples and shrimp were placed in ice, transferred to the laboratory and stored at -20 °C prior to analysis. The fish samples and shrimp were dissected with a clean plastic knife and a part of the muscle was taken out quickly. The fish (platycephalus indicus) and shrimp samples were dissected with a clean plastic knife and a part of the muscle was taken out quickly. Then it was dried in an oven at 70 °C for 48 h.

Analysis were accomplished according to the procedure reported by f Yilmaz (2003).[37] A porcelain mortar was used to grind the dried tissues. 0.5 g of each sample was digested with 5 mL of concentrated HNO_3 in Teflon beakers for 4 h at 100°C. The content was filtered into a 25 mL standard volumetric flask and was diluted up to 25 mL with double distillated water. Sediment samples were collected using a Peterson grab sampler, stored in a plastic bag in ice, transferred to the laboratory and kept at -20 °C before analysis. One gram of these samples was digested with 6 mL of HCl (37%) and 2 mL of HNO_3 (65%) in a microwave digestion system. Digestion was carried out for 2 min at 250 W, 2 min at 0 W, 6 min at 250 W, 5 min at 400 W, 8 min at 550 W and then venting for 8 min. After acid digestion was completed, the acid digests were diluted up to 100 mL with double distilled water.

2.6.2. Reference material

The concentration of Cd(II) and Ni(II) ions was determined at optimum conditions in a standard reference material (Sea food mix 02-2932). The standard material was digested according to the mentioned procedure for fish and blank digestion. The pH of the solution was adjusted to 6.4 for the separation and preconcentration of Cd(II) and Ni(II) ions form the solution. Ultimately, the preconcentration procedure mentioned above was applied to the resulted solutions.

2.7. Experimental design methodology

In order to thoroughly investigate the effect of the experimental variables that can significantly influence the extraction procedure, individual factors must be considered along with nonlinear effects and interaction terms. A rational experimental design is a kind of chemometric approach, which allows simultaneous variation of all experimental factors, reduces the required time and

number of trials which subsequently results in the reduction of the overall required costs. The Box–Behnken design (BBD) is probably the most widely used experimental design applied for fitting a second-order response surface. This cubic design is characterized by a set of points lying at the midpoint of each edge of a multidimensional cube and center point which can be replicated whereas the 'missing corners' help the experimenter to avoid using the combined factor extremes. This property prevents a potential loss of data.[40]

In this study the StatGraphics plus 5.1 package was used for the analysis of the experimental design data and calculating the predicted responses.

3. Results and discussion

3.1. Characterization studies

3.1.1. FT-IR spectra and elemental analysis

The FT-IR spectrum of the modified Fe_3O_4@SiO_2 NPs was recorded using KBr pellet method. The advent of the absorption peaks at 3412 cm^{-1} (N–H), 1583 cm^{-1} (C=N) and 1479 cm^{-1} (C=C) proposed the existence of PPy on the surface of Fe_3O_4@SiO_2 NPs (Fig. 1S, Electronic Supplementary Data). Moreover, elemental analysis revealed the presence of 0.52% N in the structure of the Fe_3O_4@SiO_2 NPs. This data indicates that Fe_3O_4@SiO_2 NPs had been successfully modified with PPy.

3.1.2. Transmission and scanning electron microcopies

The morphological structure of Fe_3O_4@SiO_2@PPy NPs was studied by SEM. As it is illustrated in Fig. 2a, the spherical structure of Fe_3O_4 NPs was approximately preserved after modification

with PPy. Furthermore, The SEM micrograph confirmed that the magnetic sorbent are nano-sized with an average particle size of 50 nm. Also the morphology of Fe_3O_4@SiO_2@PPy NPs was characterized by TEM (Fig. 2b). Fig 2b demonstrates that Fe_3O_4 nanoparticles were successfully coated by a thin layer of SiO_2. In this figure, two regions with different electron densities can be distinguished which confirms the formation of the core-shell structure: [33] an electron dense region which corresponds to Fe_3O_4 cores with a uniform size of about 15-20 nm and a less dense and more translucent region surrounding these cores that is SiO_2 and PPy coating shell with a thickness of about 10-15 nm.

3.1.3. X-ray diffraction

The structure of Fe_3O_4@SiO_2@PPy NPs was analyzed by an X-ray diffractometer and the results are shown in Fig. 3. As can be seen from the x-ray pattern, all of the diffraction peaks of Fe_3O_4@ SiO_2@PPy show that the sketch of the Fe_3O_4 crystal is well retained even after the modification with PPy. Also seven characteristic diffraction peaks appeared at 2θ = 30.1°, 35.5°, 43.2°, 53.8°, 57.1°, 62.6° and 74.7° are corresponding to (220), (311), (400), (422), (511), (440) and (622) Bragg diffractions of face centered cubic structured Fe_3O_4 core. Moreover, the diffraction peak appeared at 2θ = 17.3° is related to PPy. [35] The average crystallite size of Fe_3O_4@SiO_2@PPy NPs was estimated from the XRD pattern using Scherrer formula:

$$D = \frac{k\lambda}{\beta \cos \theta}$$

where D is the average crystallite size, λ is the X-ray wavelength, β is the full-width at half maximum (FWHM) and θ is the diffraction angle. Here K = 0.9 is chosen for spherical shape. So

the crystallite size of Fe_3O_4@SiO_2@PPy NPs was computed from XRD pattern and found to be about 60 nm.

3.2. Optimization of the preconcentration procedure

3.2.1. Sorption step

The optimization step for the uptake of metal ions on the magnetic nanosorbent was carried out using Box-Behnken design (BBD). Variables affecting the extraction efficiency were chosen to be: pH, amount of the magnetic nanosorbent, and extraction time. Other parameters involved in the extraction were kept constant, particularly the concentration of heavy metal ions (0.5 mg L^{-1}). This design permitted the responses to be modeled by fitting a second-order polynomial, which can be expressed as the following equation:

$$\boldsymbol{Y = \beta_0 + \beta_1 x_1 + \beta_2 x_2 + \beta_3 x_3 + \beta_{12} x_1 x_2 + \beta_{13} x_1 x_3 + \beta_{23} x_2 x_3 + \beta_{11} x_1^2 + \beta_{22} x_2^2 + \beta_{33} x_{13}^2}$$

where, x_1, x_2, and x_3 are the independent variables, β_0 is an intercept, β_1- β_{33} are the regression coefficients, and Y is the response (removal% or recovery%). The number of experiments (N) is then defined by the expression below:

$$\boldsymbol{N = 2K\,(K - 1) + C_o}$$

where K is the number of variables and C_o is the number of center points.[28] In this study, K and C_o were both set at 3, which meant that 15 experiments had to be done. The levels of each factor are listed in Table 1. The results of the analysis of variance (ANOVA) produced the Pareto chart of main and interaction effects which is shown in Fig. 3a. The standard effect was estimated for

computing the t-statistic for each effect. The vertical line on the plot shows statistically significant effects. The bar extracting beyond the line corresponds to the effects that are statistically significant at 95% confidence level.[40,41] Furthermore, the positive or negative sign (corresponding to a colored or colorless response) can enhance or reduce the extraction efficiency, respectively, while increasing from the lowest to the highest level set for that specific factor. According to the Pareto chart the pH of the solution causes the most significant positive effect on the extraction efficiency. The uptake of heavy metal ions increases as the pH value increases. In less acidic solutions, the uptake is quite low. This observation is due to the protonation of the magnetic nanosorbent active sites especially, the N atoms of PPy. As the pH increases, the protonation of these active sites decreases and the condition becomes more favorable for complex formation and sorption of the heavy metal ions to the magnetic nanosorbent. The response surface methodology (RSM) (Fig. 3b) was applied to analysis simultaneous effects of the extraction time and pH value on the response plot that displayed the interaction between these independent variables. The sorption efficiency of target metal ions increased along with the increase in pH. Moreover, the extraction time and the sorbent amount both showed positive effect on the extraction efficiency and were the second and third important factors, respectively. According to the overall results of the optimization study, the following experimental conditions were chosen: pH, 6.4; extraction time, 6.0 min; amount of the magnetic sorbent, 30 mg.

3.2.2 Selection of eluent

In this work several acidic eluents including HCl, HNO_3 and $HClO_4$ solutions were examined as the elution solvent. Other factors were kept constant during the optimization (pH, 6.4; extraction

time, 6.0 min; the magnetic sorbent amount, 30 mg; eluent volume, 4 mL; elution time, 20 min). Results showed that HNO_3 can recover the target metal ions. In the next step the effect of HNO_3 volume and concentration were optimized.

3.2.3. Elution step

Three factors were studied in the elution step using experimental design: eluent volume (mL), elution time (min), and eluent concentration (mol L^{-1}). In this condition, a response surface design could be performed without previously performing a screening design. The BBD was chosen because it requires the least number of experiments (15 run). The data obtained were evaluated by ANOVA. The results of the experimental design were evaluated at 5% of significance and analyzed by standardized Pareto chart (Fig. 4a). Based on BBD, both the concentration and volume of the eluent showed positive and significant effect on the recovery of the target metal ions while elution time has a positive but non-significant effect. These observations are most possibly due to increased protonation of the hetero atoms of the sorbent as the concentration of the eluent increases and also fast kinetics of elution process is of great importance. As Fig. 4a shows, eluent volume has the greatest influence on the extraction recovery. The RSM (Fig. 4b) was applied to analyze simultaneous effects of the elution time and eluent concentration on the responses. The extraction efficiency of target ions increased along with an increase in the eluent concentration and also elution time. According to the overall results of the optimization study, the following experimental conditions were chosen as the optimized ones: eluent volume, 7.5 mL; elution time, 14.5 min; and eluent concentration, 1.5 mol L^{-1} HNO_3 solution.

3.3. Effect of breakthrough volume

For the analysis of real samples, the sample volume is one of the important parameters affecting the preconcentration factor. Hence, the breakthrough volume of sample solutions was investigated by dissolving 1 mg of each Cd(II) and Ni(II) ions in 250, 500, 750, 1000, 1250, 1500, and 1750 mL distilled water. Then, the SPE protocol was carried out and the results demonstrated that the dilution effect was not significant for sample volumes of 1500 mL for both of these ions on the magnetic nanosorbent. It was concluded that the simultaneous quantitative recovery of Cd(II) and Ni(II) ions on the magnetic sorbent can be obtained for sample volumes up to 1500 mL. Thus, the new nanosorbent enabling an enrichment factor of 200 was obtained for Cd(II) and Ni(II) ions.

3.4. Effect of the potentially interfering ions

In order to investigate the effect of the potentially interfering ions found in natural samples, various metal ions were added to 100 mL of a solution containing 0.01 mg Cd(II) and 0.01 mg Ni(II) ions. The degree of tolerance for potentially interfering ions is presented in Table 1S (Electronic Supplementary Data, ESM). From the tolerance results, it can be seen that even high levels of the potentially interfering ions show no impact on the preconcentration of Cd(II) and Ni(II) ions at pH 6.4. So the proposed method could be applied to determine the target ions in complicated matrix samples satisfactorily.

3.5. Sorption capacity study

In order to investigate the sorption capacity of the magnetic sorbent a standard solution containing 10 mg L^{-1} of Cd(II) and Ni(II) was used. In order to evaluate the maximum sorption

capacity, the initial and equilibrium amounts of the target metal ions were determined by FAAS. The maximum sorption capacity is defined as the total amount of heavy metal ions sorbed per gram of the magnetic nanosorbent. The obtained capacity of the magnetic nanosorbent was found to be 120 and 98 mg g^{-1} for Cd(II) and Ni(II) ions respectively.

3.6. Analytical performance of the method

Under the optimum conditions, calibration curves were gained for the determination of Cd(II) and Ni(II) ions, according to the mentioned procedure. Linearity was within the range of 1-100 ng mL^{-1} for Cd(II) and 4-150 ng mL^{-1} for Ni(II) in initial solution. The correlation of determination (r^2) was 0.996 for Cd(II) and 0.994 for Ni(II) ions. The limit of detection is defined as LOD = $3S_b/m$, where S_b is the standard deviation of 10 replicate blank signals and m is the slope of the calibration curve after preconcentration. For a sample volume of 750 mL, it was found to be 0.3 ng mL^{-1} for Cd(II) and 1.2 ng mL^{-1} for Ni(II) ions. The precision of the method for a standard solution containing 25 ng mL^{-1} of Cd(II) and Ni(II) ions (n = 3) was evaluated as the relative standard deviation (RSD%) and was found to be 6.9 and 8.8%, for Cd(II) and Ni(II) ions respectively.

3.7. Validation of the method

The concentration of Cd(II) and Ni(II) ions obtained by the current method were compared to the exact concentration of the target ions in standard reference materials. For this reason, the concentration of the heavy metal ions was determined at optimum conditions in standard reference material (Sea food mix 02-2932). As it can be seen in Table 2, good correlation was obtained between the estimated content by the present method and the real amount the mentioned

ions in reference material. Therefore, the magnetic nanosorbent can be used as a reliable solid phase for the extraction and determination of Cd(II) and Ni(II) ions in various samples.

3.8. Determination of Cd(II) and Ni(II) ions in various real samples

Since natural samples have complex matrices, non-specific background absorption is always caused by interfering species of the sample matrix. To reduce this undesirable effect, the magnetic nanosorbent was applied for the selective extraction of Cd(II) and Ni(II) ions at pH 6.4. Table 3 shows the Cd(II) and Ni(II) ions' recoveries in various real samples which in all cases, were almost quantitative.

4. Conclusion

A simple, fast, reproducible, and selective magnetic solid-phase extraction procedure, based on Fe_3O_4@SiO_2@PPy nanocomposite, has been developed for determining Cd(II) and Ni(II) ions. The modification of the sorbent helps it to show selectivity towards these heavy metals. In comparison with other solid-phases, the magnetic sorbent exhibits the advantages of excellent sorption capacity, low limit of detection, and high enrichment factor (Table 2S, Supplementary information). Also it has been shown that the RSDs of the present method are similar to those of other methods. Hence, the analytical performance of this method is acceptable. Other advantages of this method are: low time-consumption due to the magnetically-assisted separation of the sorbent and high surface area; therefore, satisfactory results can be achieved using fewer amounts of the sorbent. Due to the relatively high preconcentration factor, trace amounts of heavy metals at trace levels in high-volume samples can be quantified by the magnetic nanosorbent.

Acknowledgements

The authors would like to thank Young Researchers and Elite Club, Tabriz Branch, Islamic Azad University, Tabriz, Iran, for the financial support of this research.

References

[1] U. Farooq, M.A. Khan, M. Athar, J.A. Kozinski, *Chem. Eng. J.*, 2011, **171**, 400-410.

[2] J.N. Bianchin, E. Martendal, R. Mior, V.N. Alves, C.S.T. Araújo, N.M.M. Coelho, E. Carasek, *Talanta*, 2009, **78**, 333-336.

[3] N.M. Kalariya, B. Nair, D.K. Kalariya. N.K. Wills, F.J.G.M.V. Kuijk, *Toxicol. Let.*, 2010, **198**, 56-62.

[4] W. Guo, S. Hu, Y. Xiao, H. Zhang, X. Xie, *Chemospher*, 2010, **81**, 1463-1468.

[5] J. Kristiansen, J.M. Christensen, T. Henriksen, N.H. Nielsen, T. Menne, *Anal. Chim. Acta*, 2000, **403**, 265-272.

[6] D. Bohrer, P. Cícero do Nascimento, M. Guterres, T. Trevisan, E. Seibert, *Analyst*, 1999, **124**, 1345-1350.

[7] Y.-H. Sung, S.-D. Huang, *Anal. Chim. Acta*, 2003, **495**, 165-176.

[8] E.L. Silva, P. dos Santos Roldan, M.F. Giné, *J. Hazard. Mater.*, 2009, **171**, 1133-1138.

[9] C. Duran, H.B. Senturk, L. Elci, M. Soylak, M. Tufekci, *J. Hazard. Mater.*, 2009, **162**, 292-299.

[10] J. Yin, Z. Jiang, G. Chang, B. Hu, *Anal. Chim. Acta*, 2005, **540**, 333-339.

[11] B. Zawisza, R. Sitko, *Spectrochim. Acta B Atomic Spect.*, 2007, **62**, 1147-1152.

[12] P. Bruno, M. Caselli, G. Gennaro, P. Ielpo, T. Ladisa, C.M. Placentino, *Chromatographia*, 2006, **64**, 537-542.

[13] S. Abe, K. Fuji, T. Sono, *Anal. Chim. Acta*, 1994, **293**, 325-330.

[14] J. Chen, K.C. Teo, *Anal. Chim. Acta*, 2011, **450**, 215-222.

[15] M.M. Matlock, B.S. Howerton, D.A. Atwood, *Water Res.*, 2002, **36**, 4757-4764.

[16] M.C. Yebra-Biurrun, A. Bermejo-Barrera, M.P. Bermejo-Barrera, M.C. Barciela-Alonso, *Anal. Chim. Acta*, 1995, **303**, 341-345.

[17] M. Faraji, Y. Yamini, A. Saleh, M. Rezaee, M. Ghambarian, R. Hassani, *Anal. Chim. Acta*, 2010, **659**, 172-177.

[18] A. Duran, M. Tuzen, M. Soylak, *J. Hazard. Mater.*, 2009, **169**, 466-471.

[19] M. Tuzen, M. Soylak, L. Elci, *Anal. Chim. Acta*, 2005, **548**, 101-108.

[20] M. Tuzen, K.O. Saygi, M. Soylak, *J. Hazard. Mater.*, 2008, **156**, 591-595.

[21] A.A. ALOthman, M. Habila, E. Yilmaz, M. Soylak, *Microchim. Acta*, 2012, **177**, 397-403.

[22] M. Tuzen, K.O. Saygi, C. Usta, M. Soylak, *Bioresource. Technol.*, 2008, **99**, 1563-1570.

[23] M. Tuzen, K.O. Saygi, M. Soylak, *J. Hazard. Mater.*, 2008, **152**, 632-639.

[24] M. Taghizadeh, A.A. Asgharinezhad, N. Samkhaniany, A. Tadjarodi, A. Abbaszadeh, M. Pooladi, *Microchim Acta*, 2014, **181**, 597-605.

[25] J.S. Suleiman, B. Hu, H. Peng, C. Huang, *Talanta*, 2009, **77**, 1579-1583.

[26] H. Parham, N. Pourreza, N. Rahbar, *J. Hazard. Mater.*, 2009, **163**, 588-592.

[27] M. Faraji, Y. Yamini, S. Shariati, *J. Hazard. Mater.*, 2009, **166**, 1383-1388.

[28] M.R. Sohrabi, Z. Matbouie, A.A. Asgharinezhad, A. Dehghani, *Microchim. Acta*, 2013, **180**, 589-597.

[29] M. Taghizadeh, A.A. Asgharinezhad, M. Pooladi, M. Barzin, A. Abbaszadeh, A. Tadjarodi, *Microchim. Acta*, 2013, **180**, 1073-1084.

[30] M. Ghaemi, G. Absalan, *Micochim. Acta*, 2014, **181**, 45-53.

[31] M. Faraji, Y. Yamini, M. Rezaee, *Talanta*, 2011, **81**, 831-836.

[32] H. Bagheri, A. Afkhami, M. Saber-Tehrani, H. Khoshsafar, *Talanta*, 2012, **97**, 87-95.

[33] M. Helmi, R. Farimani, N. Shahtahmassebi, M.R. Roknabadi, N. Ghows, *Nanomed. J.*, 2014, **1**, 71-78.

[34] A.A. Asgharinezhad, H. Ebrahimzadeh, M. Rezvani, N. Shekari, M. Loni, *Food Addit. Contam.*, 2014, **31**, 1196-1204.

[35] T. Yao, T. Cui, X. Fang, J. Yu, F. Cui, J. Wu, *Chem. Eng. J.*, 2013, **225**, 230-236.

[36] S. Weijie, C. Ping, Y. Ye, C. Yang, T. Qin, Z. Shan, high-magnetic heavy-metal ion adsorbent carrying conductive high molecules and preparation method thereof, CN 101708463 B, 2010.

[37] A.B. Yilmaz, *Environ. Res.*, 2003, **92**, 277-281.

[38] S. Sadeghi, E. Aboobakri, *Microchim. Acta*, 2012, **178**, 89-97.

[39] E. Sahmetlioglu, E. Yilmaz, E. Aktas, M. Soylak, *Talanta*, 2014, **119**, 447-451.

[40] G.E.P. Box, N.R. Draper, *Empirical Model Building and Response Surfaces*, John Wiley and Sons, New York, 1987.

[41] StatGraphics Plus 5.1 for Windows, Statistical Graphic Crop., online manuals, 2001.

[42] M. Faraji, Y. Yamini, A. Saleh, M. Rezaee, M. Ghambarian, R. Hassani, *Anal. Chim. Acta,* 2010, **659**, 172-177.

Figure captions

Fig. 1: A schematic diagram for the synthesis of Fe_3O_4@SiO_2@PPy magnetic nanocomposite.

Fig. 2: (a) The SEM image and (b) The TEM image of the Fe_3O_4@SiO_2@PPy magnetic nanocomposite.

Fig. 3: The High-angle X-ray diffraction pattern of Fe_3O_4@SiO_2@PPy magnetic nanocomposite.

Fig. 4: (a) Pareto chart of the main effects in the BBD (sorption step). AA, BB and CC are the quadratic effects of pH, the extraction time and the amount of the magnetic sorbent, respectively. AB, AC and BC are the interaction effects between pH and the extraction time; pH and the amount of sorbent and the extraction time and the amount of magnetic sorbent, respectively. (b) RSM obtained by plotting pH *vs.* extraction time using the BBD.

Fig. 5: (a) Pareto chart of the main effects in the BBD (elution step). AA, BB and CC are the quadratic effects of the elution time, eluent concentration and eluent volume, respectively. AB, AC and BC are the interaction effects between elution time and eluent concentration; elution time and eluent volume; and eluent concentration and eluent volume, respectively. (b) RSM obtained by plotting elution concentration *vs*. eluent volume.

Fig. 1

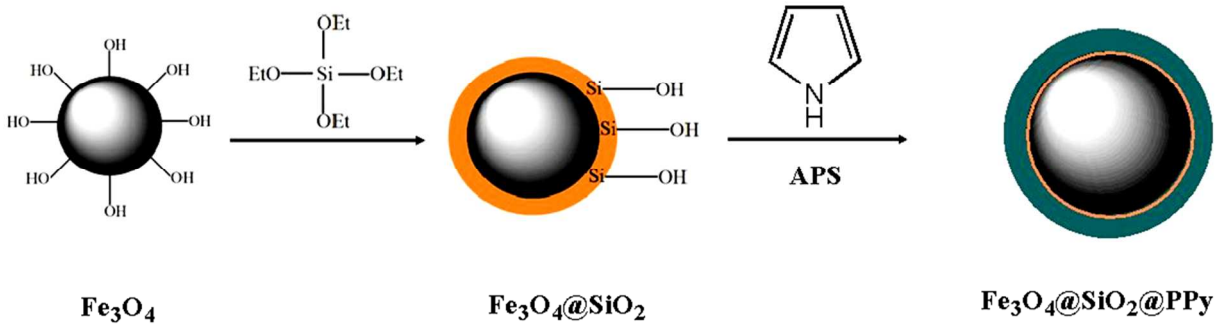
OH
HO
OH
HO
OH
HO
OH
OH
OEt
EtO
Si
OEt
OEt
Si
OH
Si
OH
Si
OH
N
H
APS
Fe_3O_4
$Fe_3O_4@SiO_2$
$Fe_3O_4@SiO_2@PPy$

Fig. 2

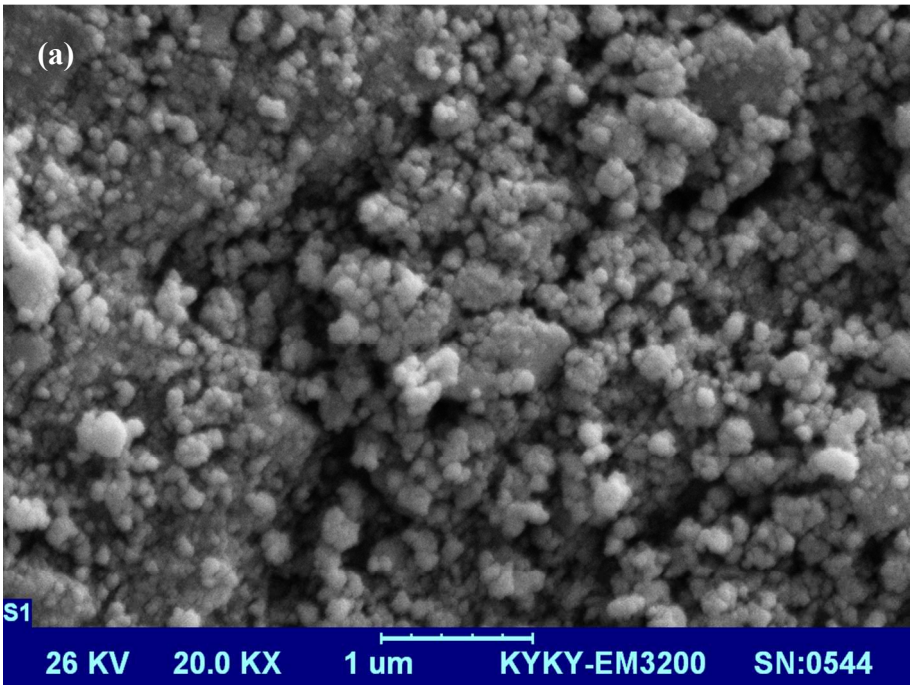

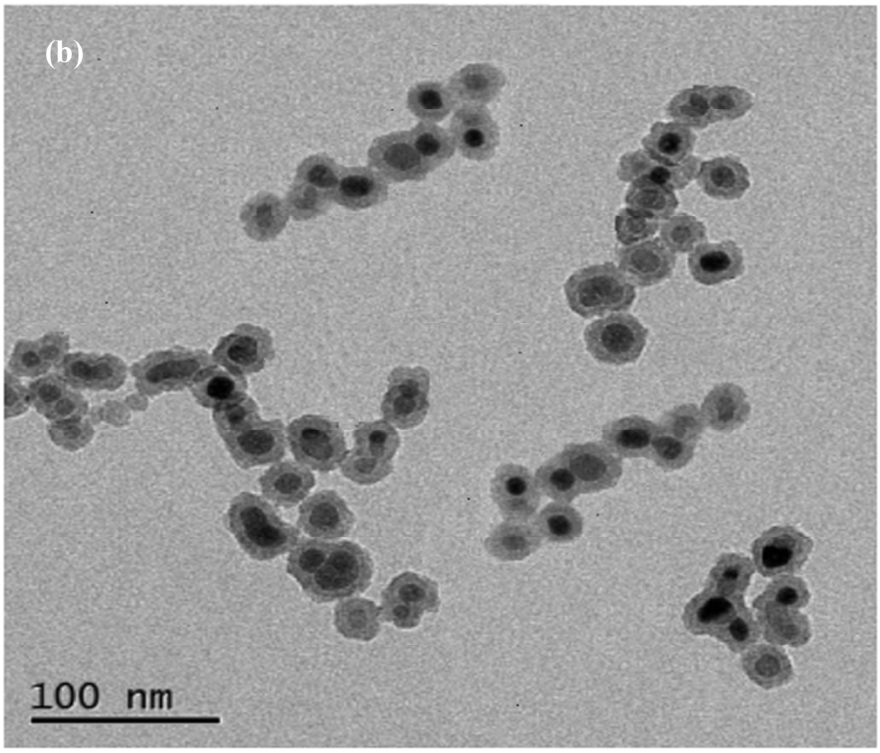

Fig. 3

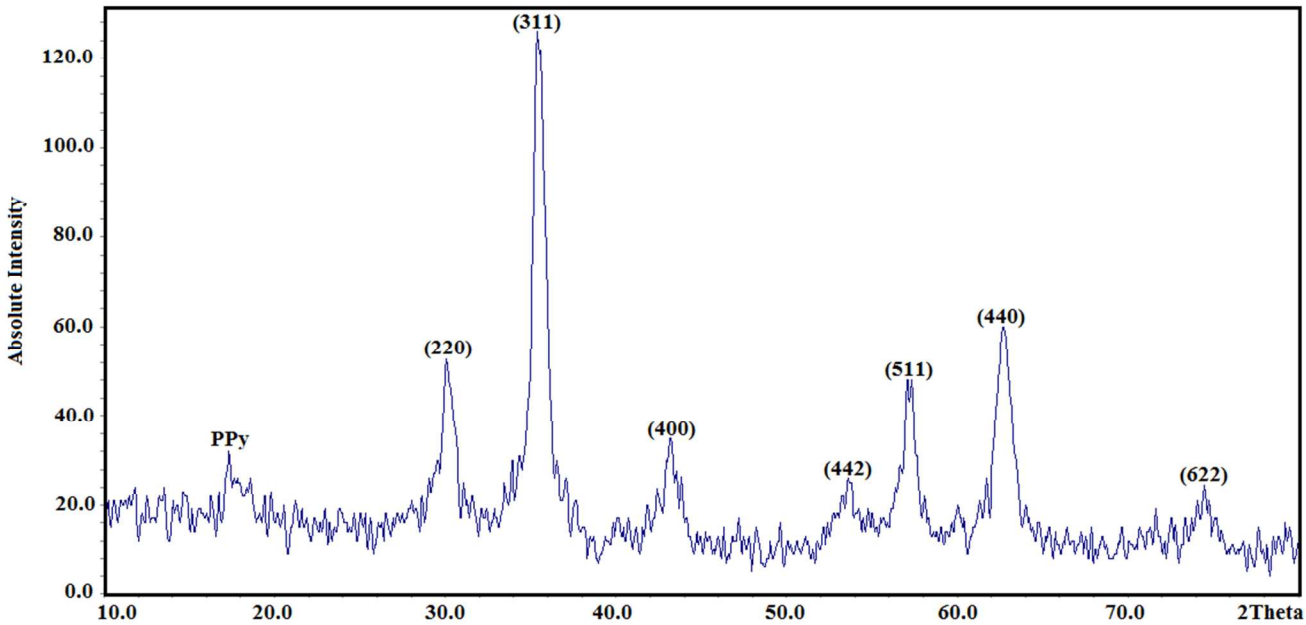
(311)
120.0
100.0
80.0
60.0
40.0
20.0
0.0
Absolute Intensity
(220)
PPy
(400)
(442)
(511)
(440)
(622)
10.0
20.0
30.0
40.0
50.0
60.0
70.0
2Theta

Fig. 4

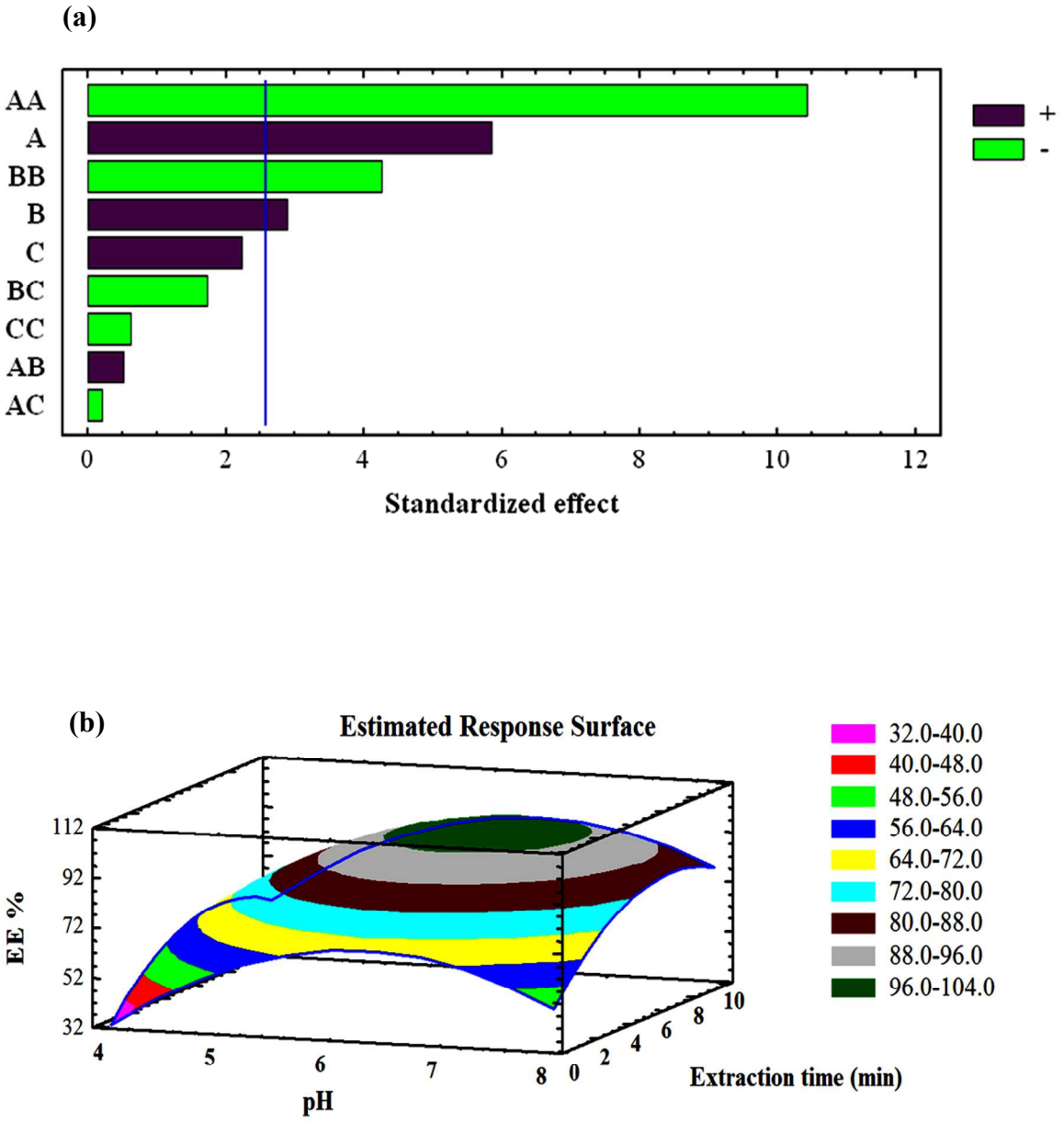
(a)
AA
A
BB
B
C
BC
CC
AB
AC
0
2
4
6
8
10
12
Standardized effect
+
-
(b)
Estimated Response Surface
112
92
72
52
32
EE %
4
5
6
7
8
pH
0
2
4
6
8
10
Extraction time (min)
32.0-40.0
40.0-48.0
48.0-56.0
56.0-64.0
64.0-72.0
72.0-80.0
80.0-88.0
88.0-96.0
96.0-104.0

Fig. 5

(a)

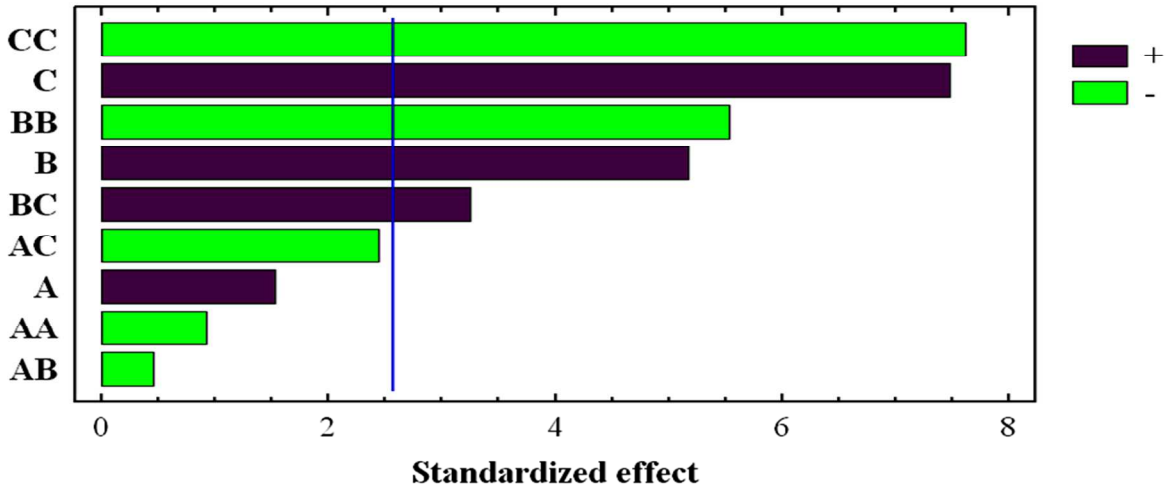
CC
C
BB
B
BC
AC
A
AA
AB
0
2
4
6
8
Standardized effect
+
-

(b)

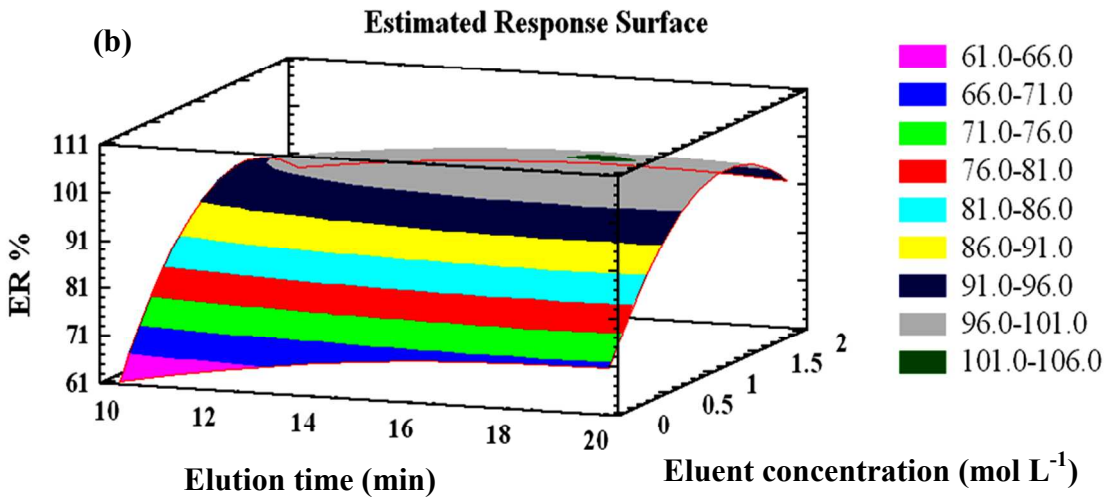
Estimated Response Surface
ER %
111
101
91
81
71
61
10
12
14
16
18
20
Elution time (min)
0
0.5
1
1.5
2
Eluent concentration (mol L-1)
61.0-66.0
66.0-71.0
71.0-76.0
76.0-81.0
81.0-86.0
86.0-91.0
91.0-96.0
96.0-101.0
101.0-106.0

Table1. Experimental variables and levels of the Box Behnken design (BBD).

		Level		
		Lower	Central	Upper
Sorption step	A: pH	4.0	6.0	8.0
	B: Uptake time (min)	2.0	6.0	10
	C: Magnetic sorbent amount (mg)	20	30	40
Elution step	A: Elution time (min)	10	15	20
	B: Eluent concentration (mol L^{-1})	0.1	1.05	2.0
	C: Eluent volume (mL)	2.0	6.0	10

Table 2
Determination of Cd(II) and Ni(II) in a certified reference material.

Sample	Concentration (mg kg^{-1})			Relative error %
	Element	Certified	Found	
Sea food mix	Cd	4.764	4.63	-2.8
	Ni	3.071	2.90	-5.6

Table 3
Determination of Cd(II) and Ni(II) ions in different real samples.

Sample	Element	Real sample (ng g^{-1})	Added (ng g^{-1})	Found (ng g^{-1})	Recovery (%)
Fish (Behad creek)	Cd	6.7	10	15.6	89.0
	Ni	21.3	10	30.5	92.0
Fish (Jafare creek)	Cd	8.8	10	18.7	99.0
	Ni	60.5	10	71.4	109
Shrimp	Cd	15.0	10	23.7	87.0
	Ni	49.3	10	57.6	83.0
Canned tuna	Cd	5.1	10	14.6	95.0
	Ni	40.1	10	48.5	84.0
Fish (Caspian Sea)	Cd	19.6	10	29.0	94.0
	Ni	98.4	10	107	86.0
Fish (Siahroud River)	Cd	32.2	10	41.5	93.0
	Ni	25.3	10	36.0	107